CHAPTER ONE

Linking microbial body size to community co-occurrences and stability at multiple geographical scales in agricultural soils

Pengfa Li[a,b], Alex J. Dumbrell[c], Muhammad Saleem[d], Lu Kuang[a], Ting Li[a], Lu Luan[b], Weitao Li[e], Guilong Li[b], Meng Wu[b], Baozhan Wang[a], Jiandong Jiang[a], Ming Liu[b,*], and Zhongpei Li[b,*]

[a]Department of Microbiology, Key Lab of Microbiology for Agricultural Environment, Ministry of Agriculture, College of Life Sciences, Nanjing Agricultural University, Nanjing, China
[b]State Key Laboratory of Soil and Sustainable Agriculture, Institute of Soil Science, Chinese Academy of Sciences, Nanjing, China
[c]School of Life Sciences, University of Essex, Colchester, Essex, United Kingdom
[d]Department of Biological Sciences, Alabama State University, Montgomery, Alabama, United States
[e]CAS Key Laboratory of Tropical Forest Ecology, Xishuangbanna Tropical Botanical Garden, Chinese Academy of Sciences, Menglun, Mengla, Yunnan, China
*Corresponding authors: e-mail address: mliu@issas.ac.cn; zhpli@issas.ac.cn

Contents

Advances in Ecological Research, Volume 67
ISSN 0065-2504
https://doi.org/10.1016/bs.aecr.2022.09.002

Abstract

Body size determines individuals' life history and metabolic rates and thus, regulates community-level dynamics. However, whether body size mediates community co-occurrences and stability, especially in complex communities across different microbial trophic levels, remains unknown. Here, we investigate whether body size determines the co-occurrence pattern and stability of microbial communities across local, regional, and continental scales in the paddy soil ecosystems.

Soil samples were collected from rice paddy fields at multiple spatial scales, and soil microbial communities were subsequently sequenced. The microorganisms were then divided into different groups based on taxonomic information at phylum/subphylum level, and the average body size of each microbial group was identified based on propagule size from documented literature. We examined the relationships between microbial body size and various community traits such as potential migration rate, co-occurrence pattern, cohesion, and community stability.

Our results consistently showed that the small-sized microorganisms such as bacteria had significantly higher niche breadth, niche overlap and migration rate at various spatial scales. We found that microbial body size is consistently negatively correlated to negative co-occurrences and community stability. Our results, for the first time, put microbial body size into a broader community ecology framework, and contribute to a greater understanding of how microbial taxa with different body sizes would respond to future changes and perturbations.

1. Introduction

The functions and services of complex natural ecosystems are dependent on a relatively stable microbiome (Cramer and Katz, 2021), which is defined as the degree of variation or rate of turnover in the microbial communities (Tripathi et al., 2018). Understanding the determinants of community stability is highly important to sustain the functions and services delivered by ecological communities (Chen et al., 2021). Ecological stability is influenced by multiple biological features of microbial communities, which nevertheless depends on microbial traits and their cumulative effects on ecosystem functions, from individual- to community- level attributes (Schnabel et al., 2019). Microbial species are characterized by numerous ecological, physiological, and molecular traits and there is an emerging interest in understanding whether they have a role in microbiome functioning (Green et al., 2008; Martiny et al., 2015; McGill et al., 2006). Among these, cell size (hereafter body size) is a key eco-physiological trait that determines life history, metabolism, physiology, and many other aspects of an organism's ecology (Saleem et al., 2013). For example, larger microorganisms (protists or fungi) may have a relatively narrow niche breadth, whereas the niche breadth of smaller microorganisms (bacteria) may be

relatively wider (Luan et al., 2020), though empirical evidence is required to confirm this prediction. In addition, a significant relationship between body size and community assembly is a general and widespread pattern in macroecology (plants, animals) (Dumbrell, 2019; Farjalla et al., 2012; Luan et al., 2020). However, whether body size determines community stability at different microbial trophic levels such as bacteria, protists, and fungi, remains unknown.

The ecological pyramids demonstrate the abundance, distribution, and biomass (including individual body-sizes) of different organisms across a hierarchy, and thus, they reveal striking regularities among species and ecological communities (Jacquet et al., 2020). Similar to higher trophic pyramids, smaller microorganisms such as bacteria generally have much higher population density than larger ones such as protists and fungi within microbial trophic levels (Jacquet et al., 2020). While, the dynamic behaviour of microbial groups and systems are determined by intrinsic density-dependent phenomena such as, growth, reproduction, species interactions, and mortality (Trosvik et al., 2010). For example, the density-dependent mortality maintains the diversity and stability of microbial communities (Blazewicz et al., 2020), whereas quorum sensing (QS), a mechanism of microbial species communication also depends on cell density (Abisado et al., 2018). The density-dependent factors are likely to influence microbial community dynamics and stability, though these remain understudied (LaManna et al., 2017). But nevertheless, trophic and non-trophic interactions, space constraints, virulence, and toxin production may also determine the size and stability of microbial communities (Georgiou et al., 2017). Given that smaller organisms have faster growth rates and higher population densities than larger ones (Lindmark et al., 2018), the stronger effects of predation, mortality, antagonisms, competitive exclusion, and other environmental filters (local carrying capacities) on their densities are expected (Faust and Raes, 2012). Meanwhile, the differences in the body size of microbial taxa and their relative abundance may also determine microbial niche overlap. Therefore, we assume that smaller rather than larger-sized microbes would demonstrate more niche overlap and resultantly, they would have higher negative co-occurrences and cohesions (an index indicating the degree of connectivity of microbial species in the community) (Herren and McMahon, 2017) among species in the community.

The influence of body size in ecological interactions that maintain communities, such as antagonism, synergism (competition, facilitation, mutualism), and predation, is apparent (Zaneveld et al., 2017; Zhou and Ning, 2017), though mostly reported in the ecology of macroorgansims.

We do not know yet whether these body-size dependent species-interactions regulate stability in the natural communities of soil microbes (Saleem et al., 2013). As predicted from both theoretical and empirical studies, negative or antagonistic interactions may promote community stability (Coyte et al., 2015; de Vries et al., 2018). In addition to the species co-occurrence and cohesion patterns, community stability may also be influenced by many other factors such as microbial stress tolerance, physiological plasticity, dormancy, stochastic gene expression, dispersal rate, and species diversity, etc. (Shade et al., 2012). These aspects may also be microbial body size-dependent. Given that small-sized microorganisms may have greater physiological plasticity, survival strategies, and dispersal rates (Shade et al., 2012), and thus they may demonstrate a higher community stability, though this assumption has never been tested.

Here, we seek to test the following hypotheses: 1) negative co-occurrences would be more prevalent among smaller- compared with larger-sized microbes across microbial trophic levels; and 2) smaller- rather than larger-sized microbial taxa would demonstrate wider niche breadth, greater niche overlap, and higher community stability (Fig. 1). To test our hypotheses, we studied soil microbial communities in rice-paddy ecosystems at local, regional, and continental scales, while considering the potential spatial-scale dependencies. As the general term "stability" is multifaceted, we define community stability as the degree of structural variations in the microbial communities over space (i.e. variability), according to the "ecological checklist" of stability statement (Grimm and Wissel, 1997; Shade et al., 2012). This definition is more relevant to this research because we only intend to compare the degree of spatial structure changes between different microbial groups, rather than focusing on the response of individual microbial groups to a disturbance. Therefore, we

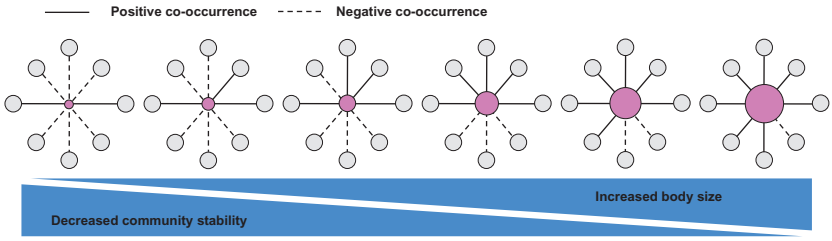

Fig. 1 Hypothetical illustration of microbial co-occurrence patterns and community stability as a function of a gradient in microbial body size. The pink circles represent the size of different microorganisms, and the grey circles represent all other microorganisms. Increasing microbial body size would reduce negative co-occurrences among microbes and promote positive co-occurrences, which ultimately would lead to community instability. Solid and dashed lines represent positive and negative co-occurrences, respectively.

calculated average Bray-Curtis dissimilarity as a proxy for predicting community stability, in the sense that a **higher** average Bray-Curtis dissimilarity should indicate a **lower** community stability over space and vice versa (Zaneveld et al., 2017).

2. Methods

2.1 Sample sites and data collection

At the **local scale**, the soil samples were collected from Yingtan Red Soil Ecological Experiment Station (28°15′30″ N, 116°55′30″ E; Fig. 2), Chinese Academy of Sciences in Yujiang County, Jiangxi Province of China. This site has a typical subtropical monsoon climate with a mean annual temperature of 17.6 °C and an annual precipitation of 1795 mm. The sampling field was a double-cropped rice (*Oryza sativa* L.) cropping system that included early and late season rice. Planting dates were early April to late October, and the rest of the year was fallow. Before the early cultivation season of 2019, five soil cores (5 cm × 10 cm × 18 cm, free from rice roots) were collected using a W-shaped transect from each plot and then pooled to form one composite sample. In total, twenty-seven soil samples were collected. The distance between any two samples is less than 100 m. Samples were stored at −40 °C until further processing.

At the **regional scale**, soil samples were collected near the end of December 2017 from red paddy soils in Yujiang (Jiangxi Province, China - 116°41′ E to 117°09′ E, and 28°04′ N to 28°37′ N; Fig. 2), where >85% of the cultivated land is paddy fields. Sampling sites were chosen to satisfy the following conditions: 1) the whole region needed to be covered; 2) the main parent material of the soils needed to be included; and, 3) field management including cropping system and fertilizer applications should be uniform. Based on these principles, twenty-six sites were selected, with pairwise geographical distances ranging from 1.3 km to 50.7 km (Fig. 2). The soil samples were collected after the harvest and in the absence of water flooding. Within each site, five soil cores (5 cm × 10 cm × 18 cm, free from rice roots) were collected using a W-shaped transect from each plot and then pooled to form one composite sample. All samples were stored at −40 °C before further processing.

At the **continental scale**, the data were collected from a published article, which quantified the soil microbiome of paddy fields (Fig. 2) (Jiao et al., 2020). Briefly, 122 rice soil samples ranging from 18.30°N to 48.35°N and 87.61°E to 99.91°E across Eastern China were collected in July–September 2017.

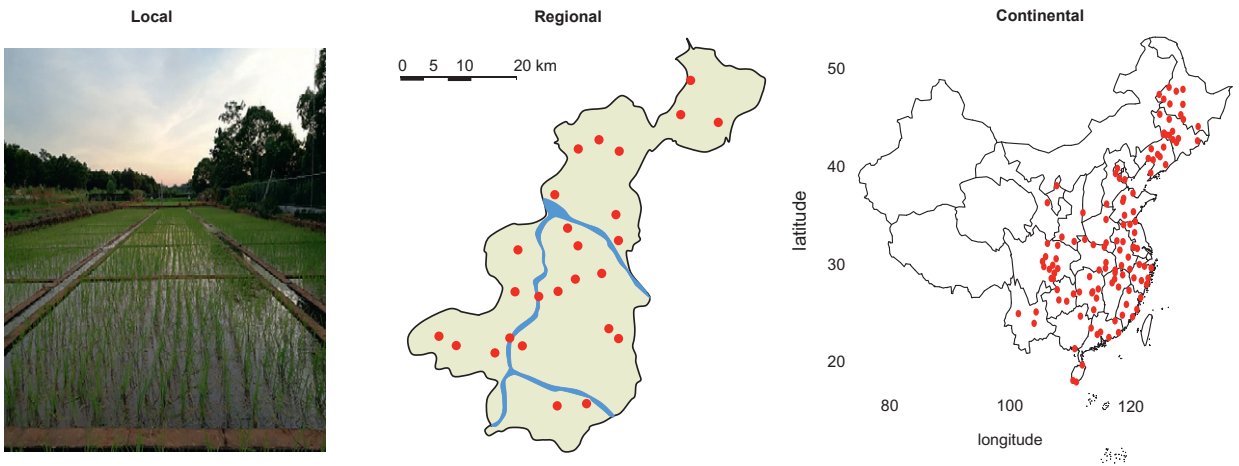

Fig. 2 Sampling sites at local, regional, and continental scale. The red dots represent sampling locations.

2.2 Molecular methods, metabarcoding and bioinformatics

For samples at local and regional scales, the soil DNA was extracted from 0.5 g of soil (fresh weight) using a Fast®DNA SPIN Kit (MP Biomedicals, CA, USA) and then subsequently purified using a PowerClean® DNA Clean-up Kit (MoBio, CA, USA) according to the manufacturers' instructions. The concentration and quality of the extracted DNA were measured using a NanoDrop ND-1000 spectrophotometer (NanoDrop Technologies, DE, USA). Three commonly used primer sets were applied to metabarcode microbial communities, targeting bacterial 16S rRNA genes (Biddle et al., 2008), the fungal ITS (Gardes and Bruns, 1993), and protist 18S rRNA genes (Stoeck et al., 2010), respectively. Detailed information about primers and PCR conditions for each primer set are shown (Table 1). The purified amplicons were pooled in equimolar concentrations, and then sent for paired-end sequencing on an Illumina MiSeq (300 bp × 300 bp) at Majorbio Bio-Pharm Technology Co. Ltd. (Shanghai, China).

For continental-scale data, raw sequences (protists were not sequenced) were downloaded from NCBI Sequence Read Archive (SRA) using the SRA toolkit "*prefetch*", and the sequences were then transformed to *fastq* format for downstream analyses using the SRA toolkit "*fastq-dump*".

Raw sequence data were analysed using the Quantitative Insights into Microbial Ecology (QIIME) pipeline (v1.9.1) (http://qiime.org/) (Caporaso et al., 2010). Paired-end reads were merged using the FLASH (Magoc and Salzberg, 2011). Reads with length of <200 bp or with average quality scores of <25 were removed. The UPARSE software was used for chimera removal, and operational taxonomic units (OTUs) were clustered at 97% sequence similarity and a representative sequence of each OTU was selected and used for taxonomic assignments (Edgar, 2013). The taxonomic identity of the bacteria, fungi, and protist OTUs was determined based on comparisons against the RDP (http://rdp.cme.msu.edu/) (Wang et al., 2007), UNITE (v7) (https://unite.ut.ee/) (Nilsson et al., 2019), and PR2 databases (http://bigd.big.ac.cn/) (Guillou et al., 2013) respectively using the RDP naïve Bayesian classifier. It should be noted that some non-protist OTUs originating from other eukaryotes were removed from the 18S datasets. The OTU data were rarefied for all microbial groups to an even sequencing depth (6677 sequences per sample) based on the sample with the minimum numbers of reads (McKnight et al., 2019).

2.3 Determination of microbial body sizes

The body-size data for species-level taxonomic assignation and/or morphological descriptions does not exist for most microbes. Thus, we distinguished

Table 1 Detailed information about primers and PCR conditions

	Primers	Primer sequence (5′- 3′)	Target gene	Target subfragment	PCR reaction condition
Bacteria	Forward: 515F	GTGCCAGCMGCCGCGGTAA	16S	V4-V5	An initial denaturation at 95 °C for 3 min, followed by 27 cycles of 30 s at 95 °C, annealing for 30 s at 55 °C and elongation for 45 s at 72 °C, the last step being extension at 72 °C for 10 min.
	Reverse: 907R	CCGTCAATTCCTTTGAGTTT			
Fungi	Forward: ITS1F	CTTGGTCATTTAGAGGAAGTAA	ITS	ITS1	An initial denaturation at 95 °C for 3 min, followed by 35 cycles of 30 s at 95 °C, annealing for 30 s at 55 °C and elongation for 45 s at 72 °C, the last step being extension at 72 °C for 10 min
	Reverse: ITS2	GCTGCGTTCTTCATCGATGC			
Protist	Forward: TAReukFWD1F	CCAGCASCYGCGGTAATTCC	18S	V4	An initial denaturation at 95 °C for 5 min, followed by 10 cycles of 30 s at 94 °C, annealing for 45 s at 57 °C and elongation for 60 s at 72 °C, and followed by 25 cycles of 30 s at 94 °C, annealing for 45 s at 45 °C, 47 °C, 48 °C, 49 °C, respectively and elongation for 60 s at 72 °C, the last step being extension at 72 °C for 2 min.
	Reverse: TAReukREV3R	ACTTTCGTTCTTGATYRA			

groups based on their taxonomic affiliation at the phylum or subphylum level, and their body sizes were identified based on propagule size through literature estimates. Recent research calculated the average microbial body sizes based on approximately 576 dominant genera, covering almost all common soil microbial phyla or subphyla (Luan et al., 2020). We also calculated and added average body sizes of some microbial groups based on our own OTU tables. The microbial groups and the average body sizes used in this study are shown in Table 2. We restricted our analysis to the most abundant phyla or subphyla (i.e., relative abundance >1% or very close to 1%), which assumed that the broadly defined functional traits such as body size and trophic status are generally conserved within the microbial taxa at phyla level (Geisen et al., 2015; Luan et al., 2020; Mulder and Elser, 2009; Zinger et al., 2019). Overall, we investigated 25, 32, and 22 microbial groups at local, regional, and continental scales, respectively (Table 2).

Table 2 Average body size of the selected microbial groups. The "+" and "-" represent whether the group was analysed or not at a particular spatial scale, respectively

Microbial group	Average body size (um)	Local scale	Regional scale	Continental scale
Acidobacteria	0.5	+	+	+
Actinobacteria	4	+	+	+
Alphaproteobacteria	0.4	+	+	+
Armatimonadetes	1	+	+	–
Bacteroidetes	0.5	+	+	+
Betaproteobacteria	5	+	+	+
Chlorobi	0.8	+	–	–
Chloroflexi	1.2	+	+	+
Cyanobacteria	4	+	+	–
Deltaproteobacteria	0.5	+	+	+
Gammaproteobacteria	5	+	+	+
Nitrospirae	5	+	+	+
Planctomycetes	1	+	+	+
Elusimicrobia	0.2	–	+	–
Firmicutes	3	–	+	+

Continued

Table 2 Average body size of the selected microbial groups. The "+" and "-" represent whether the group was analysed or not at a particular spatial scale, respectively—cont'd

Microbial group	Average body size (um)	Local scale	Regional scale	Continental scale
Gemmatimonadetes	0.5	–	+	+
Ignavibacteriae	5	–	+	+
Verrucomicrobia	0.5	–	+	+
Dothideomycetes	28.3	+	+	+
Eurotiomycetes	18.3	+	+	+
Leotiomycetes	12.5	+	+	+
Sordariomycetes	21	+	+	+
Basidiomycota	10	+	+	+
Mortierellomycota	14.3	+	+	+
Rozellomycota	1.1	–	+	+
Chytridiomycota	4.85	–	+	+
Glomeromycota	130	–	+	–
Cercozoa	13.8	+	+	–
Chlorophyta	18.1	+	+	–
Ciliophora	71.9	+	+	–
Conosa	40.2	+	+	–
Lobosa	22	+	+	–
Ochrophyta	40.5	+	+	–

2.4 Statistical analysis

We performed network analysis to explore the microbial co-occurrence patterns using the plugin CoNet in Cytoscape 3.5.1 (Shannon et al., 2003). Robust correlations between two OTUs were defined as those with Spearman's correlation coefficients (ρ) >0.6 and with false discovery rate-corrected at P values <0.01. With these, we constructed a correlation network in which each node represented one OTU, and each edge represented a strong and significant correlation between two nodes. The topology parameters of each network were determined in Cytoscape using the NetworkAnalyzer (Shannon et al., 2003).

We calculated the cohesion pattern to investigate community interconnectedness of each microbial group (Herren and McMahon, 2017). Briefly, we first calculated pairwise correlations between all taxa in each microbial group, and then used a null model to account for how the features of microbial datasets might affect correlations, and we subtracted these values. For each taxon, we averaged the positive and negative corrected correlations separately and recorded these values as the positive and negative connectedness values. Cohesion values were obtained by multiplying the relative abundance table by the connectedness values. Finally, we got two metrics of cohesion, corresponding to positive and negative values. Detailed mechanism and diagram generating cohesion metrics are available elsewhere (Herren and McMahon, 2017).

The Bray-Curtis dissimilarity of each microbial group was calculated in QIIME using the "*beta_diversity.py*" script to reflect community stability. Niche breadth and niche overlaps were calculated according to the Levin's niche breadth index and Levin's niche overlap index respectively (Li et al., 2020). A dominance test was used to determine the potential migration rate (m) of each microbial group (Sloan et al., 2007). The m is a parameter for evaluating the probability that a random loss of an individual in a local community would be replaced by dispersal from the metacommunity, and, therefore, it is a measure of dispersal limitation. Higher m values indicate that microbial communities have higher dispersal potential (Jiao et al., 2020). The formula is as follows:

$$Freq_i = 1 - I(1/N|N{*}m{*}pi,\ N{*}m{*}(1-pi))$$

where $Freq_i$ is the occurrence frequency of taxon i across communities; N is the number of individuals per community; m is the estimated migration rate; p_i is the average relative abundance of taxon i across communities; and I is the probability density function of beta distribution.

3. Results

3.1 Inferring microbial community structure and body size

We investigated soil microbial communities at local (27 samples), regional (26 samples), and continental scales (122 samples) using the metabarcoding data (Fig. 2). At the local scale, the metabarcoding analysis revealed 6677 sequences of bacterial, fungal, and protist communities per sample after excluding singletons and rarefying to an even depth. These sequences were

clustered into bacterial (4641), fungal (2478), and protistan (2044) OTUs, respectively. We sorted twenty-five microbial groups based on their body size, while these groups included 13 bacterial, six fungal groups and six protistan groups at a higher-level taxonomy (Table 2). These groups were used for the downstream analyses. At regional scale, the metabarcoding analysis revealed 7664 sequences of bacterial, fungal, and protist communities per sample after excluding singletons and rarefying to even depth. These sequences were clustered into 12,353 bacterial, 6634 fungal, and 1969 protistan OTUs, respectively. Thirty-two groups including 17 bacterial, 9 fungal, and 6 protistan groups were used for downstream analyses at regional scale (Table 2). At the continental scale, the metabarcoding data yielded 8315 sequences of bacterial and fungal communities per sample after excluding singletons and rarefying to even depth, but did not contain any protistan data. These sequences were clustered into 18,364 bacterial and 6166 fungal OTUs. From this data, we sorted twenty-two groups that included 13 bacterial and nine fungal groups for the downstream analyses.

In total, we studied 33 microbial groups in this study. Our results showed that body sizes of these 33 microbial groups ranged from 0.2 μm to 130 μm in the paddy soils. The bacterial cell size varied between 0.2 μm (*Elusimicrobia*) and 5 μm (*Betaproteobacteria, Gamaproteobacteria, Nitrospirae, and Ignavibacteriae*). The size of fungal spores ranged between 1.1 μm (Rozellomycota) and 130 μm (*Glomeromycota*). The size of protistan cells ranged from 13.8 μm (*Cercozoa*) to 71.9 μm (*Ciliophora*) (Table 2).

3.2 Microbial niche breadth, niche overlap, and migration rate

The bacteria consistently had significantly higher niche breadth, niche overlap, and migration rate than fungi and protists at all three spatial scales, aside from a non-significant difference in niche breadth between bacteria and protists at the regional scale (Fig. 3A-C). The protists had significantly higher niche breadth, niche overlap, and migration rate than fungi at the local scale; but at the regional scale, protists and fungi had similar niche breadth and niche breadth, and fungi had higher migration rate (Fig. 3A-C).

The microbial body size consistently negatively correlated with their niche breadth (Fig. 3D; **local scale**: $r = -0.566$, $P = 0.003$, $n = 25$; **regional scale**: $r = -0.216$, $P = 0.235$, $n = 32$; **continental scale**: $r = -0.628$, $P = 0.003$, $n = 22$) and niche overlap (Fig. 3E; **local scale**: $r = -0.582$, $P = 0.002$, $n = 25$; **regional scale**: $r = -0.573$, $P = 0.001$, $n = 32$; **continental scale**: $r = -0.455$, $P = 0.038$, $n = 22$), thus suggesting

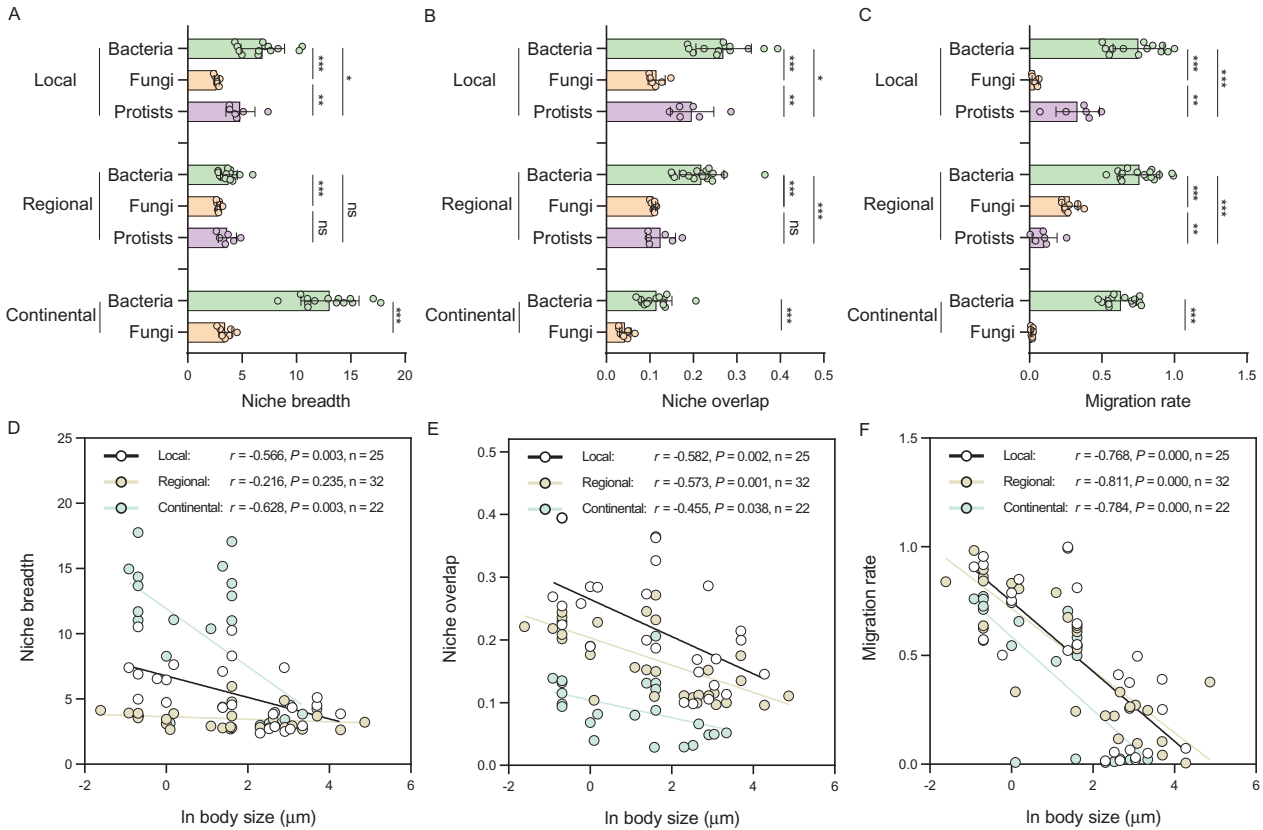

Fig. 3 See figure legend on next page.

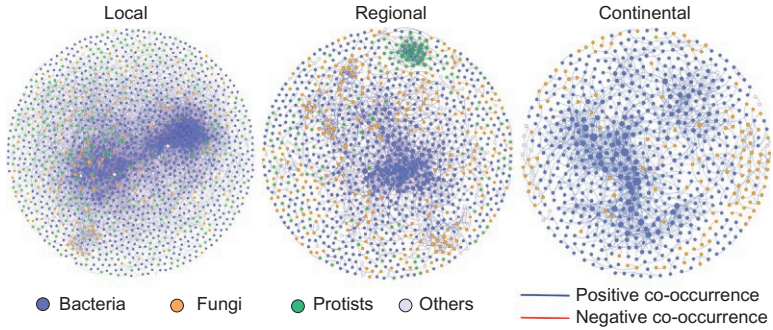

Fig. 4 Co-occurrence networks at local, regional, and continental scale. The networks were constructed under the parameters $\rho > 0.6$ and corrected *P*-values <0.01. Each node represents an OTU, and each line represents a significant and strong co-occurrence. The size of the nodes is plotted based on the total co-occurrences of each node.

that smaller-sized microbes occupy a wider niche breath, but their niches are more overlapped than the observed in larger organisms. Furthermore, our results showed that microbial body size consistently negatively correlated with the migration rate (Fig. 3F; **local scale**: $r = -0.768$, $P < 0.001$, $n = 25$; **regional scale**: $r = -0.811$, $P < 0.001$, n = 32; **continental scale**: $r = -0.784$, $P < 0.001$, n = 22).

3.3 Co-occurrence patterns of different microbial groups

We calculated co-occurrence parameters of microbial groups after constructing the multitrophic co-occurrence network (Fig. 4). Our results indicated that microbial body size was consistently negatively correlated with the average negative co-occurrences and PNC across all three spatial scales (Fig. 5A-C; **local scale**: negative co-occurrences, $r = -0.690$, $P < 0.001$, $n = 25$; PNC, $r = -0.679$, $P < 0.001$, n = 25; **regional scale**: negative

Fig. 3 Relationships between microbial body sizes and niche breadth, niche overlap, and migration rate. The average niche breadth (A), niche overlap (B), and migration rate (C) within each trophic level at various spatial scales are provided in the top row. The Relationships between microbial body sizes and niche breadth (D), niche overlap (E), and migration rate (F) at various spatial scales are provided in the bottom row. Significant differences in the niche breadth, niche overlap, and migration rate between trophic level were determined by the nonparametric Mann-Whitney *U* tests. *, **, and *** represents significant difference under $P < 0.05$, 0.01, and 0.001, respectively. 'ns' represents non-significant difference. The "n" represents the sample size of microbial groups. We applied one-side *F* and two-side *t*-tests, and then calculated *P* values as shown.

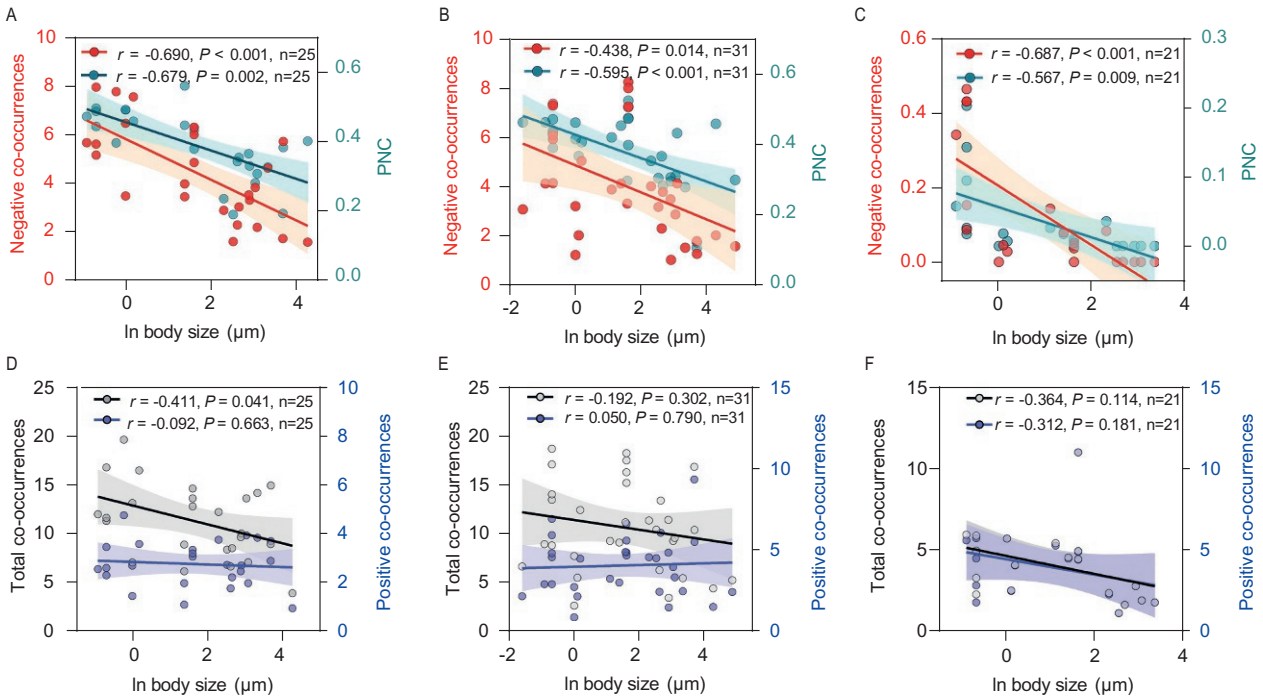

Fig. 5 See figure legend on next page.

co-occurrences, $r = -0.438$, $P = 0.014$, $n = 31$; PNC, $r = -0.595$, $P < 0.001$, n = 31; **continental scale**: negative co-occurrences, $r = -0.687$, $P < 0.001$, $n = 21$; PNC, $r = -0.567$, $P < 0.001$, n = 21). However, the correlations between microbial body size and both total and positive co-occurrences were consistently weak at all three spatial scales investigated (Fig. 5D-F).

3.4 Cohesion of differently sized microorganisms

Microbial body size was consistently positively correlated with the negative cohesion at all spatial scales (Fig. 6A-C; **local scale**: $r = 0.442$, $P = 0.027$, n = 25; **regional scale**: $r = -0.401$, $P = 0.023$, $n = 32$; **continental scale**: $r = -0.518$, $P = 0.014$, $n = 22$), thus suggesting that smaller microorganisms had consistently higher negative cohesion than larger ones. Microbial body size was also significantly negatively correlated with positive cohesion at the continental scale (Fig. 6F; $r = -0.537$, $P = 0.010$, n = 22), but not at the local or regional scales (Fig. 6D-E).

3.5 Community stability of differently sized microorganisms

The Bray-Curtis dissimilarity of each microbial group was also calculated to predict community stability, and the results showed that the microbial body size consistently positively correlated with the Bray-Curtis dissimilarity across all three spatial scales (Fig. 7; **local scale**: $r = 0.542$, $P = 0.005$, n = 25; **regional scale**: $r = 0.483$, $P = 0.005$, n = 32; **continental scale**: $r = 0.493$, $P = 0.023$, n = 22).

In addition, our results showed a significant relationship between negative co-occurrence and Bray-Curtis dissimilarity at local and regional scales, but not at the continental scale (Fig. 7; **local scale**: negative co-occurrences,

Fig. 5 Relationships between microbial body sizes and community co-occurrences. The Relationships between microbial body sizes and negative co-occurrences and PNC at local (A), regional (B), and continental (C) scales are provided in the top row. The red dots and lines indicate the relationships between microbial body sizes and negative co-occurrences, while the dark blue dots and lines describe the relationships between microbial body sizes and the PNC. The Relationships between microbial body sizes and total and positive co-occurrences at local (D), regional (E), and continental (F) scale are provided in the bottom row. The grey dots and lines indicate the relationships between microbial body sizes and total co-occurrences, while the blue dots and lines describe the relationships between microbial body sizes and the positive co-occurrences. The "*n*" represents the sample size of microbial groups. We applied one-side *F* and two-side *t*-tests, and then calculated *P* values as shown.

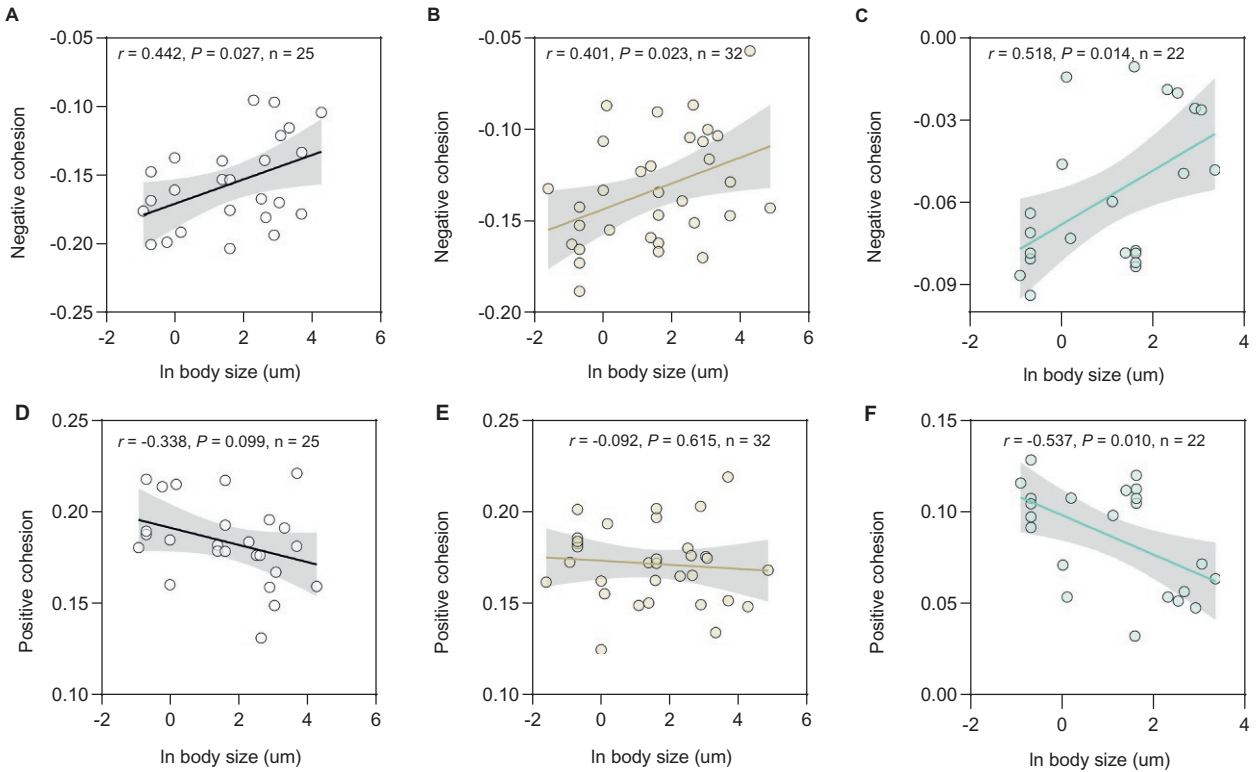

Fig. 6 Relationships between microbial body sizes and community cohesion. The Relationships between microbial body sizes and negative cohesion at local (A), regional (B), and continental (C) scale are provided in the top row. The Relationships between microbial body sizes and positive cohesion at local (D), regional (E), and continental (F) scale are provided in the bottom row. The "n" represents the sample size of microbial groups. We applied one-side *F* and two-side *t*-tests, and then calculated *P* values as shown.

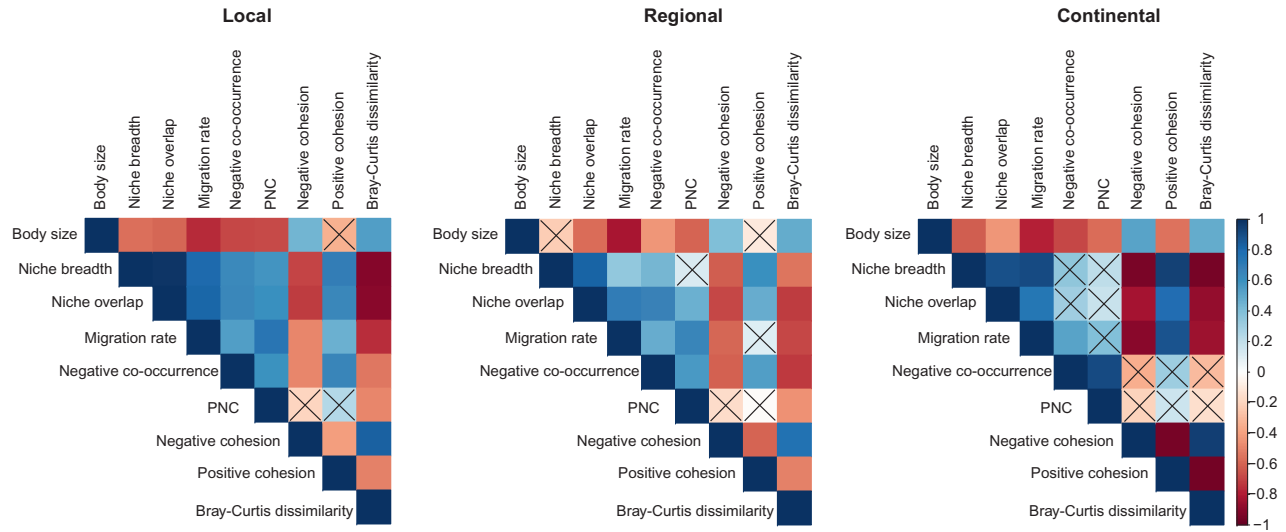

Fig. 7 The relationships of microbial body sizes and average Bray-Curtis dissimilarity at various scales. The relationship of microbial body size with niche breadth, niche overlap, migration rate, negative co-occurrences, community cohesion, and average Bray-Curtis dissimilarity at local, regional, and continental scales. We applied one-side *F* and two-side *t*-tests, and then calculated the *P* values. × represents non-significant relationship under $P < 0.05$.

$r = -0.534$, $P = 0.006$, n = 25; PNC, $r = -0.481$, $P = 0.015$, n = 25; **regional scale**: negative co-occurrences, $r = -0.722$, $P < 0.001$, n = 31; PNC, $r = -0.452$, $P = 0.011$, n = 31; **continental scale**: negative co-occurrences, $r = -0.304$, $P = 0.192$, n = 21; PNC, $r = -0.158$, $P = 0.507$, n = 21).

Furthermore, our results showed a very strong relationship between negative cohesion and Bray-Curtis dissimilarity at all three scales (Fig. 7; **local scale**: $r = 0.835$, $P < 0.001$, n = 25; **regional scale**: $r = 0.764$, $P < 0.001$, n = 32; **continental scale**: $r = 0.963$, $P < 0.001$, n = 22). Similarly, there was also a significant relationship between positive cohesion and Bray-Curtis dissimilarity at all three scales (Fig. 6; **local scale**: $r = -0.507$, $P = 0.010$, n = 25; **regional scale**: $r = -0.510$, $P = 0.003$, n = 32; **continental scale**: $r = -0.960$, $P < 0.001$, n = 22).

The microbial niche breadth, niche overlap, and potential migration rate were consistently positively correlated with the negative co-occurrences, PNC, and positive cohesion (Fig. 7). On the contrary, the niche breadth, niche overlap, and potential migration rate were consistently negatively correlated with the negative cohesion and Bray-Curtis dissimilarity at all three scales (Fig. 7).

4. Discussion

Using high-throughput sequencing and ecological models, this study discerns the role of body size in microbial co-occurrence, community cohesion, and stability patterns at local, regional, and continental scales. We show that body size is the primary determinant of microbial co-occurrence patterns and community cohesion and stability. Our results consistently demonstrated that small-sized microorganisms exhibited higher negative co-occurrences and negative cohesion, and subsequently a higher community stability across spatiotemporal scales. This study puts microbes into a common body-sized based community ecology framework that has been previously applied to the macroorganisms to determine their interactions and roles in food webs (Woodward et al., 2005).

Our results show that microbial body size consistently correlated with the average negative co-occurrences, PNC, and negative cohesion across all three spatial scales (Fig. 5, Fig. 6). These results support our first hypothesis that negative rather than positive co-occurrences and cohesion are more prevalent among small-sized microorganisms. The decreasing negative co-occurrences and negative cohesion with increasing body sizes implies

that small-sized microorganisms may experience relatively higher competition, antagonistic interactions, and predation pressure in the community (Saleem et al., 2013). For instance, our analysis indicated a significant niche overlap between small-sized microorganisms (Fig. 3), thus implying that these fast-growing microbes may demonstrate intense intra- and inter- specific competition under resource limited conditions (Allen et al., 2006; Berendsen et al., 2012). Moreover, predation exerts a fundamental selective pressure on small-sized microbes, while trophic regulation of microbial taxa may influence microbial populations and interactions (Allen et al., 2006; Saleem et al., 2013). For instance, the selective removal of certain body-sized microbial taxa may significantly reduce their population densities, while it may release other taxa from predation and competition pressures. Thus, these microbial taxa may expand their niches and population densities (Moksnes et al., 1998; Pennings, 1990). Consequently, such a trade-off could result in the evolution of novel interactions among species that may lead to strong interactions and cohesion among species in the community.

Our results also confirm our second hypothesis that microbial communities dominated by small-sized microorganisms may demonstrate a higher community stability (Fig. 7). The decreasing community stability with increasing microbial body sizes hints that smaller- as opposed to larger- sized taxa may have: (1) a wider range of strategies to adjust to a broad range of environmental conditions; and, (2) higher dispersal potential, propensity, and ecological ranges. Moreover, our results support previous empirical and theoretical predictions that smaller-sized microbes, for instance bacteria, often have a wider niche breadth than larger-sized microorganisms such as protists and fungi (Fig. 3) (Finlay, 2002; Langenheder et al., 2005; Luan et al., 2020), which nevertheless, suggests an increased niche overlap in these taxa (Fig. 3). Generalists are typically small-sized microbes with wider niche breadth, thus implying that they can frequently evolve, adapt or acclimate to changing environmental conditions (Jiao et al., 2020). In contrast, large-sized microbes with a narrower niche breadth and higher positive co-occurrences may respond in tandem to environmental fluctuations that may compromise their community stability (Coyte et al., 2015; de Vries et al., 2018). The environmental fluctuations resulting from locally less favourable conditions, can cause mass effects that may be more prominent on the large-sized taxa with narrow niches and limited dispersal propensity (Shmida and Wilson, 1985). Moreover, dispersal potential is a size-dependent factor that may influence community stability. Although historically microorganisms are categorized as non-dispersal limited or cosmopolitan, recent research has consistently

challenged this narrative (Farjalla et al., 2012). In a manner consistent with recent predictions (Luan et al., 2020), we found a significant decrease in the dispersal potential in the large-sized microorganisms such as protists and fungi (Fig. 3), suggesting the expectation that these taxa might be more sensitive to climate and land-use change (Saleem and Moe, 2014). A higher dispersal propensity of smaller-sized microorganisms would potentially homogenize microbial populations, thus creating similar microbial communities across different patches and scales (Fodelianakis et al., 2019). However, we could not directly link a given taxon's dispersal potential to the microbial negative co-occurrence patterns. This is most likely because highly motile organisms that can rapidly disperse into the surrounding environment are less likely to interact with other individuals of the same species, either via competition or cooperation (Hibbing et al., 2010; Reichenbach et al., 2007).

The co-occurrence and connectivity of microbial taxa have been previously hypothesized to influence the community dynamics (Coyte et al., 2015; Nilsson and McCann, 2016), and our study clearly demonstrated that community "negative patterns" especially negative cohesion can well predict the community's stability. Our results are in line with findings from a previous study on phytoplankton communities in the Lake Mendota, which also reported a significant relationship between negative cohesion and community stability (Herren and McMahon, 2017). These results may well indicate that negative interactions (as indicated by either co-occurrences or cohesion indices) between microbial species are arranged non-randomly to interact with each other, thereby stabilizing the community composition. While, the strong negative interactions between microbial species would act as a buffer as opposed to a source of community variations. From the perspective of correlation parameters, the negative cohesion (Fig. 7; r ranges from 0.764 to 0.963) may be more powerful than negative co-occurrences (Fig. 7; r ranges from -0.304 to -0.722) in predicting microbial community stability. This is possibly because the co-occurrence network analysis only considers significant and strong correlations between microbial taxa, whereas the cohesion index considered all pairwise correlations between microbial taxa. Natural ecosystems are always dominated by many weak interactions and a few strong interactions, while these prevalent weak interactions are also ecologically important in affecting community variation and stability (McCann et al., 1998). Therefore, the co-occurrence network analysis overlooks these important weak and intermediate interactions, resulting in a relatively weak correlation between network parameters and community stability.

On the contrary, all possible interactions, either weak, intermediate or strong, are considered in the cohesion matrix (Herren and McMahon, 2017), strengthening its power in predicting community stability.

We acknowledge that correlation between community stability and "negative patterns" might also be related to species diversity (Shade et al., 2012), which has not been taken into consideration in this study. This is because comparing species diversity at phylum or class level using metabarcoding sequencing is not a tractable and representative method as we cannot rarefy all investigated microbial groups into an even sequencing depth. However, not considering diversity does not affect our conclusions regarding microbial co-occurrence and cohesion patterns because these indices were calculated using average parameters of each microbial taxon (co-occurrence), or average pairwise correlations between taxa (cohesion).

Finally, our findings robustly demonstrate that microbial "negative patterns" and community stabilities are tightly linked to their body size, irrespective of the spatial scale. Thus, this study provides the foundations for a mechanistic and predictive role of body size in microbial community ecology. Specifically, our results provide solid evidence that body size is the primary determinant of microbial co-occurrence, cohesion, and community stability in the paddy soil ecosystems across spatiotemporal scales. Meanwhile, we acknowledge that there might be discrepancies resulting from variations in the microbial sizes. Therefore, further studies testing the body-size dependent interactions in microbial communities would be required to generalize the role of body size in the microbial community ecology. Particularly, the manipulated experiments representing microbial communities of differently sized taxa at various trophic levels will further add into the understanding of microbial community assembly, co-occurrence, cohesion, and stability. Our findings also highlight the need for more accurate quantification of body sizes among microbial taxa in situ, and the integration of these data with microbial community parameters to discern the significance of body sizes in microbial community assembly and stability. Despite these various limitations, our study provides a foundation for a mechanistic understanding of microbial communities and trophic groups with respect to body size and community stability. Moreover, our results may contribute to a greater understanding of how microbial taxa with different body sizes would respond to future changes and perturbations. In particular, the results suggest the expectation that fungal and protistan taxa will be more sensitive to perturbations than bacterial communities in the agricultural soils. Overall, we anticipate that body size will determine the stability of bacterial, protist, and fungal communities at all trophic levels.

5. Data accessibility statement

Raw sequence data used in this study are archived in the NCBI Sequence Read Archive (SRA) under the accession numbers SRP260652 (16S rRNA gene sequences at local scale), SRP260858 (ITS sequences at local scale), SRP260878 (18S rRNA sequences at local scale), SRP301389 (16S rRNA gene sequences at regional scale), SRP200912 (ITS sequences at regional scale), SRP301388 (18S rRNA sequences at regional scale), and SRP199784 (16S rRNA gene sequences and ITS sequences at continental scale).

Acknowledgements

We thank the authors whose data were used in this research. This study was supported by the National Natural Science Foundation of China (42207349, 42177294), Natural Science Foundation of Jiangsu Province (BK20221005), China Postdoctoral Science Foundation (2022M711653), and Jiangsu Funding Program for Excellent Postdoctoral Talent (2022ZB331).

References

Abisado, R.G., Benomar, S., Klaus, J.R., Dandekar, A.A., Chandler, J.R., 2018. Bacterial quorum sensing and microbial community interactions. mBio 9, e01749–18.

Allen, C.R., Garmestani, A.S., Havlicek, T.D., Marquet, P.A., Peterson, G.D., Restrepo, C., Stow, C.A., Weeks, B.E., 2006. Patterns in body mass distributions: sifting among alternative hypotheses. Ecol. Lett. 9, 630–643.

Berendsen, R.L., Pieterse, C.M.J., Bakker, P.A.H.M., 2012. The rhizosphere microbiome and plant health. Trends Plant Sci. 17, 478–486.

Biddle, J.F., Fitz-Gibbon, S., Schuster, S.C., Brenchley, J.E., House, C.H., 2008. Metagenomic signatures of the Peru margin subseafloor biosphere show a genetically distinct environment. Proc. Natl. Acad. Sci. U. S. A. 105, 10583–10588.

Blazewicz, S.J., Hungate, B.A., Koch, B.J., Nuccio, E.E., Morrissey, E., Brodie, E.L., Schwartz, E., Pett-Ridge, J., Firestone, M.K., 2020. Taxon-specific microbial growth and mortality patterns reveal distinct temporal population responses to rewetting in a California grassland soil. ISME J. 14, 1520–1532.

Caporaso, J.G., Kuczynski, J., Stombaugh, J., Bittinger, K., Bushman, F.D., Costello, E.K., Fierer, N., Pena, A.G., Goodrich, J.K., Gordon, J.I., Huttley, G.A., Kelley, S.T., Knights, D., Koenig, J.E., Ley, R.E., Lozupone, C.A., McDonald, D., Muegge, B.D., Pirrung, M., Reeder, J., Sevinsky, J.R., Tumbaugh, P.J., Walters, W.A., Widmann, J., Yatsunenko, T., Zaneveld, J., Knight, R., 2010. QIIME allows analysis of high-throughput community sequencing data. Nat. Methods 7, 335–336.

Chen, L.T., Jiang, L., Jing, X., Wang, J.L., Shi, Y., Chu, H.Y., He, J.S., 2021. Above- and belowground biodiversity jointly drive ecosystem stability in natural alpine grasslands on the Tibetan plateau. Glob. Ecol. Biogeogr. 30, 1418–1429.

Coyte, K.Z., Schluter, J., Foster, K.R., 2015. The ecology of the microbiome: networks, competition, and stability. Science 350, 663–666.

Cramer, A.N., Katz, S.L., 2021. Primary production and habitat stability organize marine communities. Glob. Ecol. Biogeogr. 30, 11–24.

de Vries, F.T., Griffiths, R.I., Bailey, M., Craig, H., Girlanda, M., Gweon, H.S., Hallin, S., Kaisermann, A., Keith, A.M., Kretzschmar, M., Lemanceau, P., Lumini, E., Mason, K.E., Oliver, A., Ostle, N., Prosser, J.I., Thion, C., Thomson, B., Bardgett, R.D., 2018. Soil bacterial networks are less stable under drought than fungal networks. Nat. Commun. 9, 3033.

Dumbrell, A.J., 2019. Size matters in regulating the biodiversity of tropical forest soils. Mol. Ecol. 28, 525–527.

Edgar, R.C., 2013. UPARSE: highly accurate OTU sequences from microbial amplicon reads. Nat. Methods 10, 996.

Farjalla, V.F., Srivastava, D.S., Marino, N.A.C., Azevedo, F.D., Dib, V., Lopes, P.M., Rosado, A.S., Bozelli, R.L., Esteves, F.A., 2012. Ecological determinism increases with organism size. Ecology 93, 1752–1759.

Faust, K., Raes, J., 2012. Microbial interactions: from networks to models. Nat. Rev. Microbiol. 10, 538–550.

Finlay, B.J., 2002. Global dispersal of free-living microbial eukaryote species. Science 296, 1061–1063.

Fodelianakis, S., Lorz, A., Valenzuela-Cuevas, A., Barozzi, A., Booth, J.M., Daffonchio, D., 2019. Dispersal homogenizes communities via immigration even at low rates in a simplified synthetic bacterial metacommunity. Nat. Commun. 10, 1314.

Gardes, M., Bruns, T.D., 1993. ITS primers with enhanced specificity for Basidiomycetes - application to the identification of mycorrhizae and rusts. Mol. Ecol. 2, 113–118.

Geisen, S., Rosengarten, J., Koller, R., Mulder, C., Urich, T., Bonkowski, M., 2015. Pack hunting by a common soil amoeba on nematodes. Environ. Microbiol. 17, 4538–4546.

Georgiou, K., Abramoff, R.Z., Harte, J., Riley, W.J., Torn, M.S., 2017. Microbial community-level regulation explains soil carbon responses to long-term litter manipulations. Nat. Commun. 8, 1223.

Green, J.L., Bohannan, B.J., Whitaker, R.J., 2008. Microbial biogeography: from taxonomy to traits. Science 320, 1039–1043.

Grimm, V., Wissel, C., 1997. Babel, or the ecological stability discussions: an inventory and analysis of terminology and a guide for avoiding confusion. Oecologia 109, 323–334.

Guillou, L., Bachar, D., Audic, S., Bass, D., Berney, C., Bittner, L., Boutte, C., Burgaud, G., de Vargas, C., Decelle, J., del Campo, J., Dolan, J.R., Dunthorn, M., Edvardsen, B., Holzmann, M., Kooistra, W.H.C.F., Lara, E., Le Bescot, N., Logares, R., Mahe, F., Massana, R., Montresor, M., Morard, R., Not, F., Pawlowski, J., Probert, I., Sauvadet, A.L., Siano, R., Stoeck, T., Vaulot, D., Zimmermann, P., Christen, R., 2013. The protist ribosomal reference database (PR2): a catalog of unicellular eukaryote small sub-unit rRNA sequences with curated taxonomy. Nucleic Acids Res. 41, D597–D604.

Herren, C.M., McMahon, K.D., 2017. Cohesion: a method for quantifying the connectivity of microbial communities. ISME J. 11, 2426–2438.

Hibbing, M.E., Fuqua, C., Parsek, M.R., Peterson, S.B., 2010. Bacterial competition: surviving and thriving in the microbial jungle. Nat. Rev. Microbiol. 8, 15–25.

Jacquet, C., Gounand, I., Altermatt, F., 2020. How pulse disturbances shape size-abundance pyramids. Ecol. Lett. 23, 1014–1023.

Jiao, S., Yang, Y.F., Xu, Y.Q., Zhang, J., Lu, Y.H., 2020. Balance between community assembly processes mediates species coexistence in agricultural soil microbiomes across eastern China. ISME J. 14, 202–216.

LaManna, J.A., Belote, R.T., Burkle, L.A., Catano, C.P., Myers, J.A., 2017. Negative density dependence mediates biodiversity-productivity relationships across scales. Nat. Ecol. Evol. 1, 1107–1115.

Langenheder, S., Lindstrom, E.S., Tranvik, L.J., 2005. Weak coupling between community composition and functioning of aquatic bacteria. Limnol. Oceanogr. 50, 957–967.

Li, P.F., Li, W.T., Dumbrell, A.J., Liu, M., Li, G.L., Wu, M., Jiang, C.Y., Li, Z.P., 2020. Spatial variation in soil fungal communities across paddy fields in subtropical China. mSystems 5, e00704–19.
Lindmark, M., Huss, M., Ohlberger, J., Gardmark, A., 2018. Temperature-dependent body size effects determine population responses to climate warming. Ecol. Lett. 21, 181–189.
Luan, L., Jiang, Y.J., Cheng, M.H., Dini-Andreote, F., Sui, Y.Y., Xu, Q.S., Geisen, S., Sun, B., 2020. Organism body size structures the soil microbial and nematode community assembly at a continental and global scale. Nat. Commun. 11, 6406.
Magoc, T., Salzberg, S.L., 2011. FLASH: fast length adjustment of short reads to improve genome assemblies. Bioinformatics 27, 2957–2963.
Martiny, J.B., Jones, S.E., Lennon, J.T., Martiny, A.C., 2015. Microbiomes in light of traits: a phylogenetic perspective. Science 350, aac9323.
McCann, K., Hastings, A., Huxel, G.R., 1998. Weak trophic interactions and the balance of nature. Nature 395, 794–798.
McGill, B.J., Enquist, B.J., Weiher, E., Westoby, M., 2006. Rebuilding community ecology from functional traits. Trends Ecol. Evol. 21, 178–185.
McKnight, D.T., Huerlimann, R., Bower, D.S., Schwarzkopf, L., Alford, R.A., Zenger, K.R., 2019. Methods for normalizing microbiome data: an ecological perspective. Methods Ecol. Evol. 10, 389–400.
Moksnes, P.O., Pihl, L., van Montfrans, J., 1998. Predation on postlarvae and juveniles of the shore crab Carcinus maenas: importance of shelter, size and cannibalism. Mar. Ecol. Prog. Ser. 166, 211–225.
Mulder, C., Elser, J.J., 2009. Soil acidity, ecological stoichiometry and allometric scaling in grassland food webs. Glob. Chang. Biol. 15, 2730–2738.
Nilsson, R.H., Larsson, K.H., Taylor, A.F.S., Bengtsson-Palme, J., Jeppesen, T.S., Schigel, D., Kennedy, P., Picard, K., Glockner, F.O., Tedersoo, L., Saar, I., Koljalg, U., Abarenkov, K., 2019. The UNITE database for molecular identification of fungi: handling dark taxa and parallel taxonomic classifications. Nucleic Acids Res. 47, D259–D264.
Nilsson, K.A., McCann, K.S., 2016. Interaction strength revisited-clarifying the role of energy flux for food web stability. Theor. Ecol. 9, 59–71.
Pennings, S.C., 1990. Predator-prey interactions in opisthobranch gastropods - effects of prey body size and habitat complexity. Mar. Ecol. Prog. Ser. 62, 95–101.
Reichenbach, T., Mobilia, M., Frey, E., 2007. Mobility promotes and jeopardizes biodiversity in rock-paper-scissors games. Nature 448, 1046–1049.
Saleem, M., Fetzer, I., Harms, H., Chatzinotas, A., 2013. Diversity of protists and bacteria determines predation performance and stability. ISME J. 7, 1912–1921.
Saleem, M., Moe, L.A., 2014. Multitrophic microbial interactions for eco- and agro-biotechnological processes: theory and practice. Trends Biotechnol. 32, 529–537.
Schnabel, F., Schwarz, J.A., Danescu, A., Fichtner, A., Nock, C.A., Bauhus, J., Potvin, C., 2019. Drivers of productivity and its temporal stability in a tropical tree diversity experiment. Glob. Chang. Biol. 25, 4257–4272.
Shade, A., Peter, H., Allison, S.D., Baho, D.L., Berga, M., Burgmann, H., Huber, D.H., Langenheder, S., Lennon, J.T., Martiny, J.B., Matulich, K.L., Schmidt, T.M., Handelsman, J., 2012. Fundamentals of microbial community resistance and resilience. Front. Microbiol. 3, 417.
Shannon, P., Markiel, A., Ozier, O., Baliga, N.S., Wang, J.T., Ramage, D., Amin, N., Schwikowski, B., Ideker, T., 2003. Cytoscape: a software environment for integrated models of biomolecular interaction networks. Genome Res. 13, 2498–2504.
Shmida, A., Wilson, M.V., 1985. Biological determinants of species-diversity. J. Biogeogr. 12, 1–20.

Sloan, W.T., Woodcock, S., Lunn, M., Head, I.M., Curtis, T.P., 2007. Modeling taxa-abundance distributions in microbial communities using environmental sequence data. Microb. Ecol. 53, 443–455.

Stoeck, T., Bass, D., Nebel, M., Christen, R., Jones, M.D.M., Breiner, H.W., Richards, T.A., 2010. Multiple marker parallel tag environmental DNA sequencing reveals a highly complex eukaryotic community in marine anoxic water. Mol. Ecol. 19, 21–31.

Tripathi, B.M., Stegen, J.C., Kim, M., Dong, K., Adams, J.M., Lee, Y.K., 2018. Soil pH mediates the balance between stochastic and deterministic assembly of bacteria. ISME J. 12, 1072–1083.

Trosvik, P., Rudi, K., Straetkvern, K.O., Jakobsen, K.S., Naes, T., Stenseth, N.C., 2010. Web of ecological interactions in an experimental gut microbiota. Environ. Microbiol. 12, 2677–2687.

Wang, Q., Garrity, G.M., Tiedje, J.M., Cole, J.R., 2007. Naive Bayesian classifier for rapid assignment of rRNA sequences into the new bacterial taxonomy. Appl. Environ. Microbiol. 73, 5261–5267.

Woodward, G., Ebenman, B., Emmerson, M., Montoya, J.M., Olesen, J.M., Valido, A., Warren, P.H., 2005. Body size in ecological networks. Trends Ecol. Evol. 20, 402–409.

Zaneveld, J.R., McMinds, R., Thurber, R.V., 2017. Stress and stability: applying the Anna Karenina principle to animal microbiomes. Nat. Microbiol. 2, 17121.

Zhou, J.Z., Ning, D.L., 2017. Stochastic community assembly: does it matter in microbial ecology? Microbiol. Mol. Biol. Rev. 81, e00002–e00017.

Zinger, L., Taberlet, P., Schimann, H., Bonin, A., Boyer, F., De Barba, M., Gaucher, P., Gielly, L., Giguet-Covex, C., Iribar, A., Rejou-Mechain, M., Raye, G., Rioux, D., Schilling, V., Tymen, B., Viers, J., Zouiten, C., Thuiller, W., Coissac, E., Chave, J., 2019. Body size determines soil community assembly in a tropical forest. Mol. Ecol. 28, 528–543.